Molecular Therapy
Methods & Clinical Development
Original Article

Intramuscular Delivery of Replicon RNA Encoding ZIKV-117 Human Monoclonal Antibody Protects against Zika Virus Infection

Jesse H. Erasmus,[1,8,9,10] Jacob Archer,[1,8,9,10] Jasmine Fuerte-Stone,[1] Amit P. Khandhar,[1,8] Emily Voigt,[1] Brian Granger,[1] Robin G. Bombardi,[5] Jennifer Govero,[2] Qing Tan,[2] Lorellin A. Durnell,[2] Rhea N. Coler,[1] Michael S. Diamond,[2,3,4] James E. Crowe, Jr.,[5,6,7] Steven G. Reed,[1,8] Larissa B. Thackray,[2] Robert H. Carnahan,[5,6] and Neal Van Hoeven[1]

[1]Pre-Clinical Vaccine Development, Infectious Disease Research Institute, Seattle, WA, USA; [2]Department of Medicine, Washington University School of Medicine, St. Louis, MO 63110, USA; [3]Department of Molecular Microbiology, Washington University School of Medicine, St. Louis, MO 63110, USA; [4]Department of Pathology & Immunology, Washington University School of Medicine, St. Louis, MO 63110, USA; [5]The Vanderbilt Vaccine Center, Vanderbilt University Medical Center, Nashville, TN 27232, USA; [6]Department of Pediatrics, Vanderbilt University Medical Center, Nashville, TN 27232, USA; [7]Department of Pathology Microbiology & Immunology, Vanderbilt University Medical Center, Nashville, TN 27232, USA; [8]HDT Biocorp, Seattle, WA, USA; [9]Department of Microbiology, University of Washington, Seattle, WA, USA

Monoclonal antibody (mAb) therapeutics are an effective modality for the treatment of infectious, autoimmune, and cancer-related diseases. However, the discovery, development, and manufacturing processes are complex, resource-consuming activities that preclude the rapid deployment of mAbs in outbreaks of emerging infectious diseases. Given recent advances in nucleic acid delivery technology, it is now possible to deliver exogenous mRNA encoding mAbs for *in situ* expression following intravenous (i.v.) infusion of lipid nanoparticle-encapsulated mRNA. However, the requirement for i.v. administration limits the application to settings where infusion is an option, increasing the cost of treatment. As an alternative strategy, and to enable intramuscular (IM) administration of mRNA-encoded mAbs, we describe a nanostructured lipid carrier for delivery of an alphavirus replicon encoding a previously described highly neutralizing human mAb, ZIKV-117. Using a lethal Zika virus challenge model in mice, our studies show robust protection following alphavirus-driven expression of ZIKV-117 mRNA when given by IM administration as pre-exposure prophylaxis or post-exposure therapy.

INTRODUCTION

While the commercial application and impact of monoclonal antibodies (mAbs) is immense, the necessary quality and regulatory control associated with the complex manufacturing process poses an impediment to realizing their full potential. Currently there are over 80 licensed mAb therapeutics but only one of those, palivizumab, is used in humans as a passive-immunotherapy against a viral infection.[1,2] Given the recent emergence of several viral zoonotic diseases, such as those associated with infection by Zika virus, chikungunya virus, or Middle East respiratory syndrome virus, and the potential for outbreaks of pandemic diseases such as influenza or those yet to be identified, there is an urgent need to develop the capacity to respond swiftly to future biothreats. The current manufacturing paradigm includes recombinant immunoglobulin G (IgG) protein production in mammalian cell lines followed by a purification process that must be optimized for each target antibody. These IgG protein products then are qualified rigorously in a series of assays to characterize the many biochemical features that are important for their stability or biological activity.[3] In addition to the resulting long timeline for development of IgG protein drug products, on the order of years, these processes are costly, limiting their use in an outbreak scenario.

A possible solution to these problems is to shift the production of mAbs to the patient's own cells by delivering the desired antibody in the form of cDNA or mRNA molecules encoding the antibody IgG protein. This approach eliminates the protein manufacturing pipeline and instead uses a universal cell-free production and purification process that is independent of the encoded antibody nucleotide sequence.[4–10] However, deploying this strategy faces a major hurdle in that efficient delivery of nucleic acids in patient cells is not achieved with current technologies. While intramuscular (IM) electroporation of plasmid DNA encoding antibody genes has been effective in mice, scaling to larger animals remains a challenge. Also, the requirement for nuclear delivery of inoculated cDNA for subsequent mRNA transcription to occur poses a safety concern due to a possible risk of genome integration.[11] While delivery of DNA via adeno-associated viral (AAV) vectors improves expression in larger animals, both in

Received 9 January 2020; accepted 15 May 2020;
https://doi.org/10.1016/j.omtm.2020.06.011.

[10]These authors contributed equally to this work.

Correspondence: Jesse H. Erasmus, Pre-Clinical Vaccine Development, Infectious Disease Research Institute, Seattle, WA, USA.
E-mail: jerasmus@uw.edu

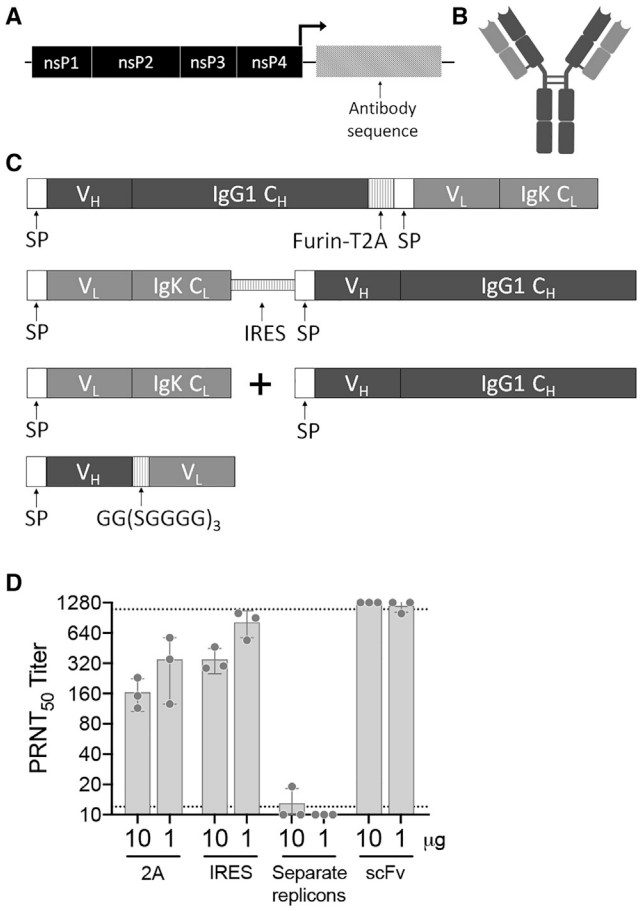

Figure 1. Expression of H and L Chains of ZIKV-117 from an Alphavirus Replicon RNA

(A) Replicon RNAs (repRNAs) derived from Venezuelan equine encephalitis virus, vaccine strain TC-83. (B) Schematic of ZIKV-117 human IgG monoclonal antibody with L and H chains depicted in light or dark gray, respectively. (C) Varied strategies for encoding ZIKV-117: a single open reading frame (ORF) separating H and L chains by a furin-T2A site; two ORFs separated by an internal ribosomal entry site (IRES); two ORFs on two separate repRNAs rep repRN; or just the variable regions expressed as an scFv. (D) 50% plaque reduction neutralization test (PRNT50) titers of supernatants harvested 24 h after transfection of BHK cells with 10 or 1 µg of various repRNAs encoding ZIKV-117. Data is representative of two independent experiments. nsP, nonstructural protein; SP, signal peptide; VH, heavy chain variable region; CH, heavy chain constant region; VL, light chain variable region; CL, light chain constant region. Data in (D) is represented as mean ± SD.

terms of peak concentrations and duration, the risk of genome integration remains.[12] In addition, AAV-mediated gene delivery faces other challenges related to immunogenicity and anti-vector immunity.[12]

More recently, mRNA has received extensive interest as a means of antibody gene delivery.[1,13,14] Advances in formulations have improved mRNA stability and delivery across the plasma membrane into the cytoplasm where protein translation can occur directly, eliminating a dependence on nuclear delivery. To date, most applications of mRNA-encoded antibodies have used an intravenous (i.v.) route of administration, targeting the highly vascularized liver or spleen in which it is easier to achieve the necessary number of transfected cells required for the expression of therapeutic levels of antibody in serum.[4,7,15–17] Disadvantages of i.v. infusions include a prolonged administration time, typically on the order of hours, as well as an estimated 50% higher treatment cost due to hospitalization or infusion center requirements compared to subcutaneous or intramuscular administration[18]. Intramuscular delivery of mRNA-encoded antibodies could enable the rapid distribution of an effective therapy to a population of individuals in an outbreak setting, but this injection route has largely failed in the past, likely due to the limited number of target cells in the inoculation site. To achieve effective expression of antibodies by RNA delivery following intramuscular administration, we used a replicating viral RNA[19] that amplifies the encoded antibody mRNA and antagonizes the innate immune response to allow for improved protein production in transfected cells.

For proof-of-principle studies of this RNA gene-delivery platform, we tested delivery of a human antibody to Zika virus (ZIKV), which has high overall public health importance because of the recent large epidemics of this viral disease.[20–23] We developed constructs to express a previously described human mAb, ZIKV-117, using alphavirus replicons. ZIKV-117 is a potently neutralizing mAb with broad activity against African and Asian lineages of ZIKV and binds a quaternary interdimer epitope on the viral envelope protein.[24,25] A recombinant ZIKV-117 mAb previously was shown to protect against lethal viral challenge in both pregnant and non-pregnant mouse models. We recently described the development of a nanostructured lipid carrier (NLC) to mediate non-viral delivery of replicon RNA (repRNA) *in vivo* as an effective strategy for developing a ZIKV vaccine.[26] Here, we adapted this platform to facilitate direct expression of ZIKV-117 mAb *in situ* following intramuscular delivery. We show high levels of mAb expression *in vivo*, which results in protection against lethal ZIKV infection in mice.

RESULTS

Alphavirus Replicon-Based Coding Strategies for the Expression of ZIKV-117

Based on previous studies of the optimization of expression of human antibodies from plasmid DNA for *in vitro* manufacturing applications,[27–29] we initially tested four different strategies in the context of alphavirus repRNA-based expression (Figure 1A). Given that canonical antibodies are comprised of heavy (H) and light (L) chains (Figure 1B), it is necessary to express both chains, using either a single open reading frame (ORF) or two separate ORFs (Figure 1C). We encoded the H- and L-chain-variable regions of ZIKV-117 as (1) a single-chain variable fragment (scFv) or (2) in an IgG1 framework as a single ORF separating the two chains by a furin and thosea asigna virus 2A (T2A) peptide sequence to promote T2A-mediated ribosomal skipping followed by host furin-mediated cleavage of residual T2A amino acids. Alternatively, (3) we used an encephalomyocarditis virus internal ribosomal entry site (IRES) sequence to mediate translation from the second ORF following cap-mediated translation of the first

ORF of the same RNA message or (4) we separated the two ORFs onto two separate repRNAs.

We then transcribed and capped these four RNA constructs and, using the NLC formulation previously described, transfected BHK21 cells with 10 or 1 μg of RNA. 24 h later, we harvested and clarified cell supernatants and measured their capacity to neutralize ZIKV in a 50% plaque reduction neutralization test ($PRNT_{50}$; Figure 1D). Whereas both the 2A and IRES strategies resulted in similar $PRNT_{50}$ titers, the separation of each ORF onto two separate repRNAs did not mediate efficient expression of neutralizing antibody, suggesting either inefficient delivery of both RNA species into the same cell or inefficient co-expression of each ORF in cells receiving both RNA species. The scFv version of ZIKV-117 was expressed more efficiently, with at least ~2-fold higher neutralizing titers at the 10 μg dose compared to the 2A or IRES strategies. Substantial cell death was observed in the groups receiving 10 μg doses of the T2A, IRES, and two repRNA IgG constructs (data not shown), whereas the same dose of the scFv construct caused less cell death. This factor likely contributes to the expression differences and suggests potential toxicity associated with expression of complete IgG compared to scFvs.

Optimization of IRES and T2A Coding Strategies *In Vitro* and *In Vivo*

Due to the short *in vivo* half-lives of scFvs and lack of Fc-mediated effector functions, we next focused on optimization of the IgG IRES and T2A strategies to maximize expression. We first evaluated the use of an IRES to drive expression of a second cistron reporter gene by screening seven viral and five cellular IRESs[30–36] in the context of an upstream antibody H-chain sequence. RepRNA constructs expressing the ZIKV-117 H chain followed by each IRES controlling the expression of nano-luciferase (nLUC) were constructed (Figure S1A). RNA was transcribed, capped, and transfected into BHK21 cells and 16 h later, cells were harvested and assayed for nLUC activity (Figure S1B). Of the viral and cellular IRESs screened, only viral IRESs mediated efficient expression of nLUC ($EMCV_{min}$ and $EMCV_{opt}$, EV71, HCV 374, CrPv).

Given this result, a subset of the viral IRESs was cloned into constructs containing either ZIKV-117 H-chain-IRES-L-chain (H-IRES-L) or L-chain-IRES-H-chain (L-IRES-H) orientations to determine the combined effect of each IRES and chain orientation on antibody expression. We transcribed and capped the RNA, transfected BHK21 cells, and 24 h later, cell supernatants were harvested and IgG was measured using an enzyme-linked immunosorbent assay (ELISA; Figure S1C). The EMCV full-length IRES produced the highest concentrations of IgG in the supernatant. When comparing antibody expression between H-IRES-L and L-IRES-H orientations, higher levels of antibody were expressed when the H chain was located in the first cistron.

We next assessed the use of two alternative signal peptides that reportedly increase antibody expression.[27] These two signal sequences, H7 and H5, were cloned onto the H-$EMCV_{opt}$-L constructs (Figure S2A), and the capped RNA was transfected into BHK21 cells. Cell supernatants were harvested 24 h later and IgG levels were measured by ELISA (Figure S2B). Significant differences were not observed between the signal sequence variants; this finding was confirmed in C57BL/6 mice (Figure S2C).

We next assessed the effect of H and L chain orientation around the IRES or T2A sequences. After generating L-$EMCV_{opt}$-H, H-$EMCV_{opt}$-L, L-T2A-H, and H-T2A-L constructs, which varied only in the relative location of the H and L chains (Figure 2A), we transfected capped RNA transcripts into BHK21 cells and measured IgG production 24 h later by western blotting of cell lysates and supernatants (Figure 2B) and ELISA of supernatants (Figure 2C). The L chain was expressed at higher relative levels than the H chain in the H-$EMCV_{opt}$-L construct in both the cell lysates and supernatants, and this finding correlated with higher IgG concentrations in the supernatant. In contrast, the L-$EMCV_{opt}$-H construct resulted in higher levels of H chain expression in cell lysates but lower IgG concentrations in the supernatants.

To confirm the unexpected observation that the IRES mediated higher levels of downstream ORF expression than the upstream cap-dependent ORF, we cloned nLUC in both orientations as H-$EMCV_{opt}$-nLUC or nLUC-$EMCV_{opt}$-H. Transcribed RNA was capped, transfected into BHK21 cells, and cell lysates were harvested 16 h later for measurement of nLUC activity (Figures S3A and S3B). Expression of nLUC downstream of the IRES in the second cistron was more efficient than cap-dependent expression from the first cistron at each of the doses tested.

In contrast to the IRES strategy, the IgG concentrations in supernatants of cells transfected with the T2A constructs were not affected by the orientation of H and L chains (Figure 2C). However, the efficiency of furin cleavage of residual T2A amino acids was affected by the upstream sequence. Furin-T2A downstream of the L chain resulted in the production and secretion of a slightly larger L chain, as observed in the western blots of cell lysates and supernatants, respectively. Whereas furin-T2A downstream of the H chain resulted in the production of a slightly larger H chain intracellularly, the supernatant appeared to contain a correctly processed form.

We performed studies in C57BL/6 mice following NLC formulation and intramuscular (IM) delivery of RNA constructs encoding ZIKV-117 mAb. First, we performed a dose escalation study to determine the maximum dose per injection that resulted in an increase in serum concentrations of ZIKV-117 mAb by formulating the RNA in NLC at 11 different RNA concentrations, while maintaining a constant nitrogen-to-phosphate ratio between NLC and RNA. We administered a single 50 μL IM injection to each group of mice (n = 3/group) such that each group received a total dose of 0, 2.5, 5, 7.5, 10, 12.5, 15, 17.5, 20, 22.5, or 25 μg of ZIKV-117 RNA. Mice were bled 5 days after injection, and the ZIKV-117 IgG protein concentration in serum was determined by ELISA (Figure S4). We

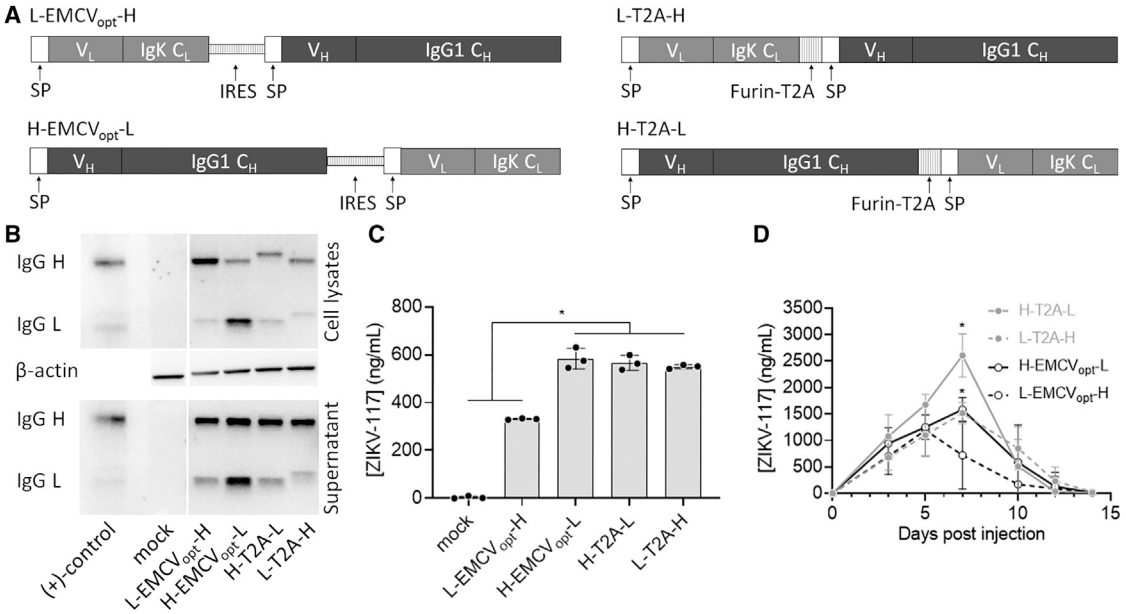

Figure 2. Optimization of H and L Chain Orientation *In Vitro* and *In Vivo*

(A) Design of IRES and Furin-T2A antibody constructs to evaluate the effect of H/L chain orientation on expression. See Figure S1 for optimization of IRES sequences. The IRES sequence depicted here is an optimized sequence derived from encephalomyocarditis virus ($EMCV_{opt}$). (B) Western blots of BHK cell lysates or supernatants 24 h after transfection with repRNAs encoding variations of ZIKV-117. Recombinant ZIKV-117 IgG protein was used as a positive control. Results are representative of 3 independent experiments. (C) Total IgG ELISAs of supernatants harvested from BHK cells 24 h after transfection with repRNAs encoding variations of ZIKV-117. *$p < 0.001$ as determined by one-way ANOVA with Tukey's multiple comparison test. Data are representative of 3 independent experiments. (D) Human anti-ZIKV IgG ELISAs of C57BL/6 (n = 8/group) mouse sera harvested at various times after IM administration of nanostructured lipid carrier-formulated repRNA encoding variations of ZIKV-117. Recombinant ZIKV-117 diluted in normal mouse serum was used to generate an absolute standard curve. *$p < 0.005$ for H-T2A-L compared to all groups and for L-T2A-H and H-$EMCV_{opt}$-L compared to L-$EMCV_{opt}$-H as determined by one-way ANOVA with Tukey's multiple comparison test at the day 7 time point. Data are representative of 2 independent experiments. Data in (C) and (D) are represented as mean ± SD.

observed increasing serum concentrations of ZIKV-117 IgG as the dose escalated from 0 to 10 μg, at which point no appreciable gains were observed suggesting a maximum RNA concentration of 200 μg/mL could be administered in a 50 μL injection volume.

Using this maximal dose per injection, we administered each of the four RNA constructs described above via the IM route in C57BL/6 mice (n = 8/group), with each mouse receiving four IM injections of 10 μg RNA for a total dose of 40 μg RNA in a single administration. We collected serum on days 0, 3, 5, 7, 10, 12, and 14 after injection and determined the levels of ZIKV-117 antibody protein by ELISA (Figure 2D). The L-$EMCV_{opt}$-H construct, which resulted in the lowest expression *in vitro* (Figure 2C), reached peak serum concentration of 1.19 μg/mL on day 5 post-injection. The H-$EMCV_{opt}$-L and L-T2A-H groups achieved similar levels on day 5 (1.25 and 1.10 μg/mL, respectively), and the H-T2A-L group reached a mean concentration of 1.68 μg/mL on day 5, which was significantly greater than L-$EMCV_{opt}$-H ($p = 0.04$; Figure 2D). Peak expression was achieved on day 7 for the H-$EMCV_{opt}$-L, H-T2A-L, or L-T2A-H groups, with mean concentrations of 1.58, 2.61, or 1.52 μg/mL, respectively, compared to the L-$EMCV_{opt}$-H group, which had declined (mean concentration of 0.72 μg/mL) to levels lower than the other groups ($p < 0.002$). The H-T2A-L group achieved significantly higher mean antibody concentration (2.61 μg/mL) compared with all other groups ($p < 0.05$). Concentrations steadily declined thereafter, and all groups exhibited a serum level of ZIKV-117 close to baseline by 14 days after injection.

RepRNA Mediates Higher Expression of Antibody Compared to Non-Replicating mRNA following IM Administration

We next constructed mRNA versions of ZIKV-117 using the H-T2A-L framework and previously published 5′ and 3′ untranslated regions, to compare repRNA-mediated antibody expression to that of non-replicating mRNA. Furthermore, we transcribed normal, as well as pseudouridine (Ψ)-modified mRNA of each construct, since previous studies demonstrated reduced innate immune stimulation by mRNAs containing pseudouridine that was associated with higher levels of protein expression.[37,38] Following transcription and capping, 40 μg of each RNA was formulated with NLC and delivered via IM injection in C57BL/6 mice, and serum was harvested on days 0, 3, 5, 7, and 10 to measure ZIKV-117 concentration by ELISA (Figure 3). RepRNA-mediated ZIKV-117 expression achieved between 17- to 32-fold higher serum concentrations of ZIKV-117 than mRNA with or without pseudouridine over the course of the experiment. Additionally, pseudouridine-modified mRNA did not improve antibody expression following IM administration. For reasons that

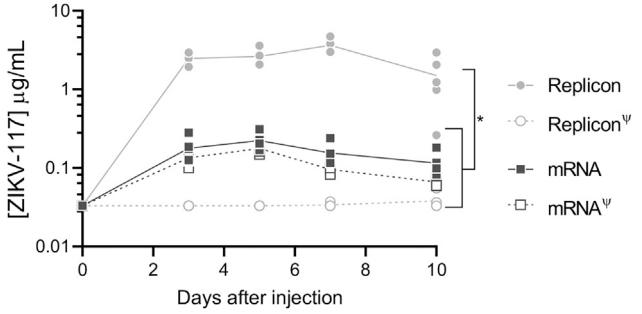

Figure 3. Comparison of repRNA and Non-Replicating mRNA *In Vivo* following IM Administration

C57BL/6 mice (n = 5/group) were injected IM with 40 μg NLC-formulated repRNA or non-replicating mRNAs, or with their pseudouridine (Ψ)-modified counterparts, each encoding ZIKV-117. ZIKV-117 concentration then was measured by ELISA in sera collected 0, 3, 5, 7, or 10 days after injection. *$p < 0.0001$ between repRNA and all other groups at all time points except day 0 as determined by two-way ANOVA with Bonferroni's multiple comparison test. Differences between mRNA and mRNA$^{\Psi}$ were not significant at all time points. Data are representative of 2 independent experiments.

remain unclear, pseudouridine-modified repRNA was non-functional, resulting in lack of detectable ZIKV-117 antibody in the serum of mice.

Rapid Protection against ZIKV Infection in Immunocompromised Mice Is Conferred by repRNA-Encoded ZIKV-117 Antibody

Although the H-T2A-L construct mediated the highest overall expression of ZIKV-117 *in vivo* (Figure 2D), we opted to evaluate the efficacy of the H-EMCV$_{opt}$-L in the context of repRNA expression using *in vivo* studies. The western blotting data suggested residual furin-T2A amino acids were present on the C terminus of the H chain in cell lysates (Figure 2B), which we reasoned might evoke an unintended immune response against the antibody. To evaluate efficacy of the H-EMCV$_{opt}$-L repRNA construct, hereafter called ZIKV-117 repRNA, we used a previously described lethal challenge model of ZIKV infection wherein a mouse-adapted (MA) strain of ZIKV (strain Dakar 41525) is combined with a single-dose antibody (MAR1-5A3[39]) blockade of type I interferon receptor (IFNAR1) to produce a lethal outcome in C57BL/6 mice.[40] We first applied this model to assess prophylactic efficacy of ZIKV-117 repRNA. C57BL/6 mice were given 2 mg of anti-IFNAR1 antibody and administered 40 μg of either ZIKV-117 repRNA or a non-specific repRNA using the same H-EMCV$_{opt}$-L framework but encoding an influenza virus-specific human antibody directed to hemagglutinin (5J8), via IM injection 1 day before challenge with 10^3 focus-forming units (FFU) of ZIKV-MA (Figure 4A). Mice then received an IM treatment of 40 μg ZIKV-117 or influenza virus-specific mAb 5J8 repRNA beginning at 1 (Figures 5A–5D) or 3 days (Figures 5E–5H) after virus inoculation. Mice were bled 1 day later to measure serum antibody concentration by ELISA (Figures 5B and 5F) and ZIKV viremia by qRT-PCR (Figures 5C and 5G). Mice were followed for survival over 21 days (Figures 5D and 5H). The mean antibody concentrations

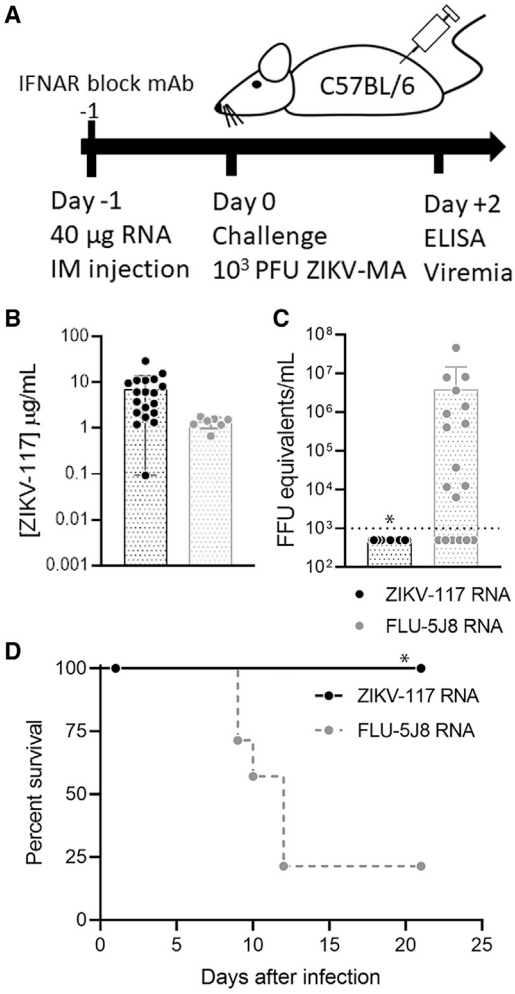

Figure 4. Rapid Prophylactic Protection against Lethal ZIKV Challenge

(A) Outline of experimental design C57BL/6 mice received i.p. injection of MAR1-5A3 antibody followed by IM administration of 40 μg of ZIKV-117 RNA. (B and C) 1 day later, mice were challenged by footpad injection with 10^3 FFU of mouse-adapted ZIKV and serum was harvested 2 days later to assess: (B) antibody concentration by ELISA and (C) viremia by qRT-PCR of extracted RNA. *$p < 0.001$ as determined by two-tailed t test. (D) Mice were monitored daily for survival until the end of the study. *$p = 0.008$ as determined by Mantel-Cox test. Results are combined from three independent experiments (n = 17 mice/group). Data in (B) and (C) are represented as mean ± SD.

in mice receiving ZIKV-117 or influenza virus-specific 5J8 repRNA therapy at day +1 after infections (2 days after infection and 3 days after MAR1-5A3 treatment) was 0.8 μg/mL and 0.6 μg/mL, respectively (Figure 5B). All mice in ZIKV-117 repRNA group were protected against detectable viremia (limit of detection = 1,000 FFU equivalents/mL; Figure 5C) and death (Figure 5D), whereas the influenza virus-specific mAb 5J8 repRNA control group experienced viremia (mean of 2.7×10^5 FFU/mL) and an 80% mortality rate. However, the cohort receiving ZIKV-117 repRNA therapy 3 days after infection had a mean human IgG concentration of 0.05 μg/mL, compared to the 5J8 control group which exhibited mean human

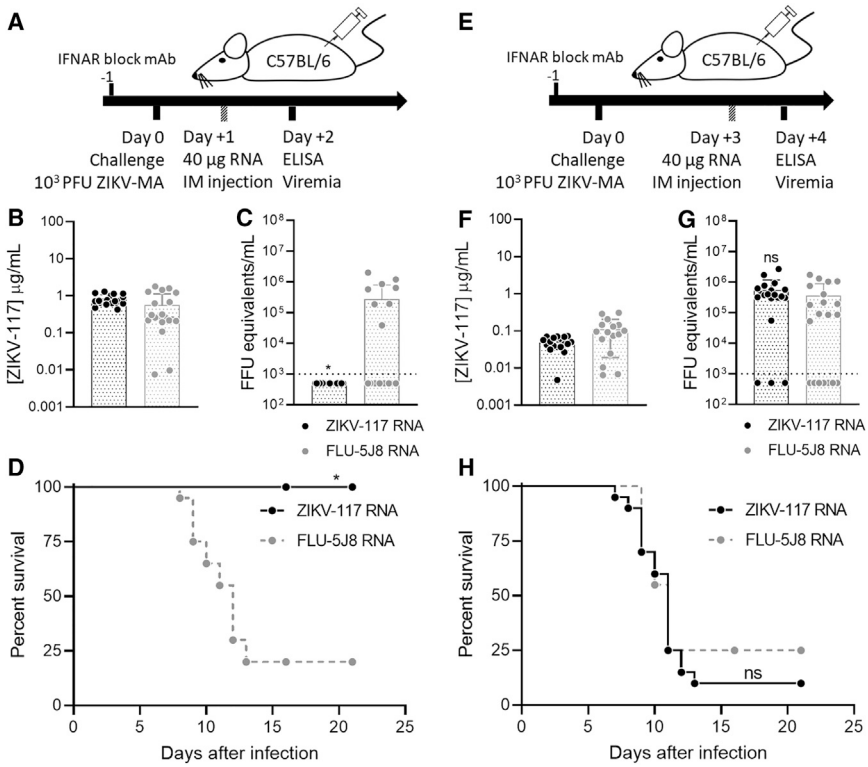

Figure 5. Therapeutic Protection against Lethal ZIKV Challenge

(A or E) Outline of experimental design. C57BL/6 mice received i.p. injection of MAR1-5A3 antibody, and 1 day later, were challenged by footpad injection with 10^3 FFU of mouse-adapted ZIKV. (A–H) Mice then received IM administrations of 40 µg of ZIKV-117 RNA either 1 (A–D) or 3 (E–H) days after RNA administration. 1 day later, serum was harvested to assess antibody concentration by ELISA (B or F), as well as viremia by qRT-PCR of extracted RNA (C or G). *p = 0.0019 as determined by two-tailed t test. Mice were monitored daily for survival (D or H) until the end of the study. *p = 0.0004 as determined by Mantel-Cox test. Results are combined from three independent experiments (n = 18 mice/group). Data in (B), (C), (F), and (G) are represented as mean ± SD.

IgG concentration of 0.1 µg/mL, 1 day after treatment (4 days after infection and 5 days after anti-IFNAR1 treatment; Figure 5F), both of which did not protect against viremia or mortality (Figures 5G and 5H). This decrease in human antibody concentration between studies is likely due to difference in ZIKV load at the time of repRNA therapy combined with increasing time from IFNAR1 blockade. The decrease in 5J8 antibody concentration can be explained by the latter, whereas the more pronounced decrease of ZIKV-117 can be explained by both factors.

Rapid Protection against ZIKV Infection in Mice Is Conferred by repRNA-Encoded ZIKV 117 Antibody Produced under Conditions of an Intact IFN Immune Response

To quantify the effect of IFNAR signaling on repRNA-mediated antibody expression, we evaluated ZIKV-117 repRNA expression kinetics in C57BL/6 mice receiving IM injections of 40 µg ZIKV-117 repRNA 1 day after mock or anti-IFNAR1 pre-treatment (Figure S5). We observed a 3- to 5-fold enhancement of antibody expression by repRNAin the presence of IFNAR1 blockade. To determine whether protection was dependent on the enhanced repRNA propagation when IFN signaling was attenuated, we evaluated whether repRNA-mediated expression of ZIKV-117 in the absence of IFNAR1 blockade could mediate protection against lethal ZIKV challenge. Given peak antibody concentrations observed between 5 and 7 days after injection of repRNAs and subsequent decline in immunocompetent mice (Figure 1D), we reasoned that the enhancing effects of IFNAR1 blockade on repRNA-mediated mAb expression would be minimal at 5 or 7 days after repRNA injection. This factor allowed us to evaluate whether antibodies expressed prior to IFNAR1 blockade could mediate protection during the immunocompromised state required for lethal endpoints in this mouse challenge model of ZIKV. In contrast to the above efficacy studies, we used an alternative and previously described[41] IFNAR1-blockade model of lethal ZIKV infection with the wild-type (WT) ZIKV Dakar strain 41525 (parental to ZIKV-MA described above) with additional low-dose MAR1-5A3 antibody administrations on days 1 and 4 after ZIKV inoculation. Using this model, two cohorts of mice (n = 8/group) were injected IM with 40 µg of ZIKV-117 RNA on either day −7 (Figures 6A–6E) or day −5 (Figures 6F–6J). Then, anti-IFNAR1 antibody was administered on days −1 and 0, and mice were bled to determine ZIKV-117 IgG concentrations immediately before challenge with 10^5 PFU of ZIKV. Additional doses of anti-IFNAR1 antibody were administered on days +1 and +4, and mice were bled to measure viremia and followed for body weight change and survival for 15 days. ELISA results from serum obtained at day 0 confirmed similar ZIKV-117 concentrations as seen in immunocompetent mice, with mean serum IgG concentration of 1.28 µg/mL from the day −7 cohort (Figure 6B; compared to 1.58 µg/mL in Figure 1D), and 1.45 µg/mL from the day −5 cohort (Figure 6G; compared to 1.25 µg/mL in Figure 1D). These levels of ZIKV-117 IgG were sufficient to reduce viremia (Figures 6D and 6I) and protect against weight loss (Figures 6C and 6H) and death (Figures 6E and 6J).

DISCUSSION

mAb countermeasures are a major strategy in the treatment and prevention of disease. Recently, the mAb therapy field has shifted toward optimization of formulations for subcutaneous delivery after evidence that a change from i.v. infusions to subcutaneous injections of trastuzumab and rituximab reduced costs and burden on the healthcare system and was preferred by patients.[42–45] Given the emerging role

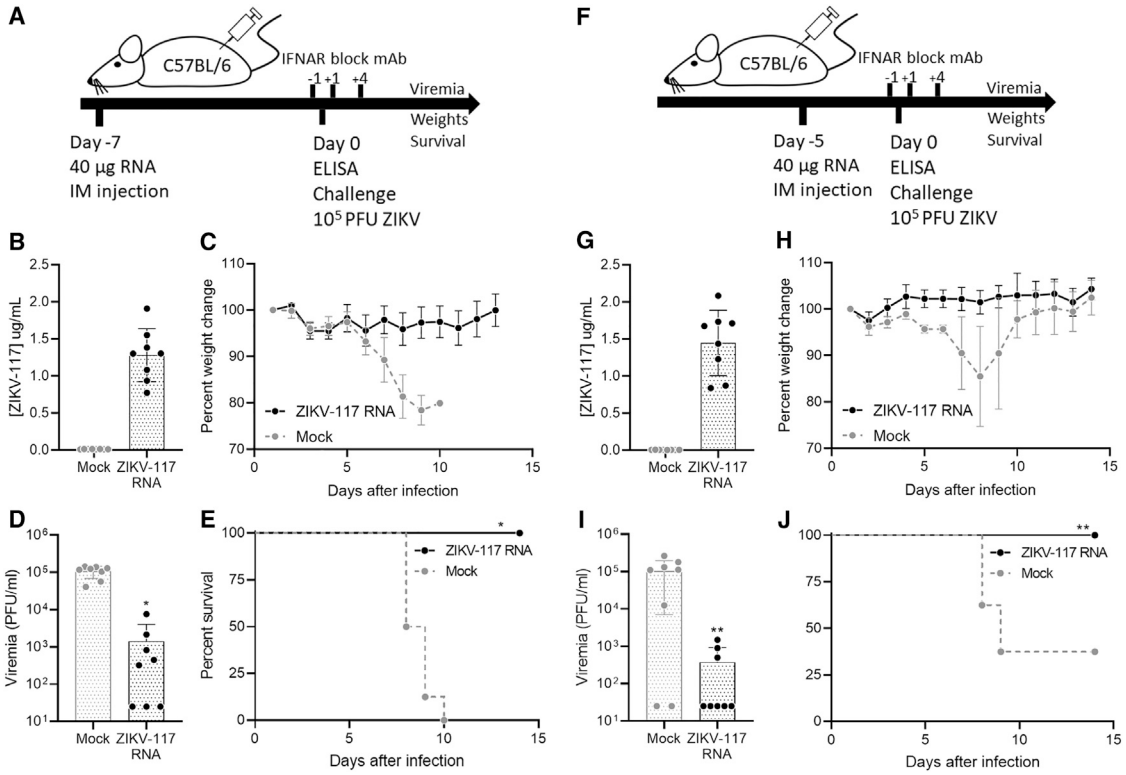

Figure 6. ZIKV-117 Expressed in the Absence of IFNAR Blocking Protects

(A or F) Outline of experimental design. (A–J) C57BL/6 mice (n = 8/group) received IM administration of ZIKV-117 RNA 7 (A–E) or 5 (F–J) days before ZIKV challenge. Mice received i.p. injection of MAR1-5A3 antibody 1 day before then 1 and 4 days after challenge. On the day of challenge, mice were bled to assess antibody concentration by ELISA and (B) then challenged by i.p. injection with 10^5 PFU of WT ZIKV. Serum was harvested 4 days after challenge to measure viremia by plaque assay (D or I). *$p < 0.0001$ and **$p = 0.007$ as determined by two-tailed t test. Mice were monitored daily for weight loss and survival (C and E or H and J) until the end of the study. *$p < 0.0001$ and **$p = 0.009$ as determined by Mantel-Cox test. Data are representative of 2 independent experiments. Data in (B), (D), (G), and (I) are represented as mean ± SD.

of mRNA gene delivery in mAb therapeutics, we aimed to develop an alternative mRNA strategy that could be administered by the IM route to avoid challenges associated with the i.v. route of administration. Furthermore, there is a need to optimize mRNA-mediated antibody gene delivery platforms for less complex routes of administration to facilitate deployment during epidemics to control outbreaks of emerging infectious diseases.[46]

Of the six studies on mRNA-encoded antibodies reported to date, five used i.v.[4,7,15–17] and one used intratracheal (IT) aerosol[6] routes of delivery. The i.v. route method primarily delivers mRNA to the liver and spleen to mediate expression of the encoded antibody, whereas the IT route can achieve local expression of antibody in the lung. The liver is an attractive target tissue for mRNA-mediated expression efforts when high serum concentration of antibody is needed, because the liver has an extensive vascular network that provides access to a large number of target cells. Alternatively, if only local expression of antibody is necessary to mediate protection at the site of infection, the number of target cells may not be a critical limiting factor. Since IM administration likely delivers mRNA to a limited number of target cells, we focused on maximizing protein secretion on a per-cell basis to achieve protective serum IgG protein concentrations. We used alphavirus-derived repRNAs, which combine self-amplification of an mRNA message encoding the antibody sequence with co-expression of viral genes that antagonize the host innate immune response.[47–50] Additionally, with a rapid-response application in mind, we used a nanostructured lipid carrier[26] to allow for independent manufacturing of the delivery formulation and target RNA, such that a stockpiled formulation could be mixed at bedside with an RNA encoding a mAb to any target prior to IM administration. In contrast to lipid nanoparticles (LNPs), which encapsulate the target RNA and require co-manufacturing of each component, NLCs bind RNA to the surface upon simple admixing.

To further improve antibody secretion from repRNA-transfected cells, we performed a series of optimization experiments, first identifying optimal signal peptides, and then screening a variety of IRES sequences in the context of repRNA-mediated expression, and finally assessing the effect of H- and L-chain orientation around the IRES or T2A intergenic sequences. While improvements between mAb ZIKV-117 repRNA constructs *in vivo* were modest (about 4-fold), we achieved serum antibody concentrations as high as 3.4 µg/mL in

immunocompetent mice following IM injection, which was sufficient to protect against death. Furthermore, 100% of mice were protected when RNA was administered 7, 5, or 1 day before and up to 1 day after challenge. Due to a growing number of reports on nucleic acid-encoded antibodies, it is worth discussing three major observations in our studies within the context of previous publications on antibodies encoded in plasmid DNA, non-replicating mRNA, and repRNA RNA, including the optimization of bicistronic constructs, the use of two monocistronic constructs, and the targeting of muscle versus liver tissue.

First, in the optimization of bicistronic expression of heterodimers of H and L chains in the context of plasmid DNA, others have established that cap-mediated translation of the L chain followed by IRES-mediated translation of the H chain (L-EMCV-H) resulted in optimal secretion of IgG from Chinese hamster ovary cells *in vitro*, resulting in a 3.8-fold improvement compared to the opposite orientation (H-EMCV-L).[28] This finding was expected given the requirement for L-chain-dependent folding of H chain and secretion of IgG monomer,[51] coupled with previous reports that IRES-mediated translation is less efficient than cap-mediated translation;[52] expression of excess L chain is favorable for IgG secretion.[53–58] However, the same finding was not observed in the context of repRNA-based expression where IRES-mediated translation was more efficient than cap-mediated translation of the upstream ORF. In this case the H-EMCV-L orientation resulted in higher peak antibody secretion *in vitro* and *in vivo*, correlating with higher expression of the L chain. This finding could be due to early IRES-mediated translation of the downstream antibody ORF directly from the repRNA genome prior to subgenomic RNA transcription-dependent expression of the upstream antibody ORF, which occurs later in the replication cycle of alphavirus repRNAs. Alternatively, alphaviruses replicate in host lipid-derived spherules where high concentrations of host and viral factors may favor IRES- rather than cap-mediated translation.[59]

Second, we were unable to express functional antibody *in vitro* upon co-transfection of two repRNAs independently encoding the H and L chains, while it has been established that plasmid DNAs or non-replicating mRNAs encoding each chain separately mediate very efficient expression of functional antibody. This finding may be due to differences in delivery formulation. Previous studies generally have used electroporation or LNPs, respectively, which could mediate efficient co-delivery of each DNA or RNA species into the same cell. In contrast, the specific conditions we used with NLC for co-transfection of two repRNA species may not have achieved efficient co-transfection. Alternatively, differences between replicating and non-replicating mRNA and DNA could explain this discrepancy. Due to the virus-like nature of repRNA, other mechanisms could be at play that inhibit the formation of monomeric IgG when each chain is encoded on a separate repRNA, such as competition between repRNAs within the same cell or host responses including endoplasmic reticulum (ER) stress.[60] As described in the results above, we did observe significant cell death in the high dose *in vitro* transfections of the IRES, T2A, and 2 repRNA constructs, while little to no cell death was observed for the scFv construct at the same dose. Perhaps expression of the H chain in the absence of, or out-of-synchrony with, expression of L chain triggers cell death via ER stress due to accumulation of H chains in the ER.[61,62] Given a dependence on L chain for secretion, H chains polymerize and sequester chaperone proteins that are involved in ER-stress signaling, such as binding immunoglobulin protein (BiP).[61,63–65] We are currently investigating the role of ER stress on repRNA-mediated secretion of antibodies from muscle cells.

Targeting muscle tissue for antibody expression poses challenges including adequate number of target cells and suitability of this cell type for secretion of large quantities of antibodies. While antibody-RNA applications mediating protection following IM administration have not been reported to date, a number of applications of plasmid DNA for *in vivo* expression of antibodies have been successful following IM electroporation. Earlier reports of IM electroporation of 100 μg plasmid DNA encoding dengue[66] or chikungunya[9] virus-specific antibodies achieved serum concentrations between 1 and 2 μg/mL. To facilitate electroporation of more target muscle cells, we pre-administered hyaluronidase with plasmid DNA to achieve better dispersal of the injection volume, resulting in serum antibody concentrations between 2 and 6.2 μg/mL following a 10 μg dose of DNA encoding either an antibody specific for influenza virus or ebolavirus.[8] A recent study combined hyaluronidase with a larger (200 μg) dose of DNA and achieved peak ZIKV serum antibody concentrations on day 14 after inoculation of 27 μg/mL in C57BL/6 mice.[5] In contrast, we achieved between 1.2 to 3.4 μg/mL serum IgG levels following a 40-μg repRNA dose split into 4 IM injections without electroporation, to reach more target cells. We plan to evaluate the use of hyaluronidase as a means to increase the maximum dose per injection.

Our experiments suggest that repRNA offers an advantage over modified or unmodified non-replicating mRNA after IM delivery, resulting in over 30-fold increase in serum concentrations of antibody. Additionally, pseudouridine-modified mRNA did not improve antibody expression *in vivo* compared to unmodified mRNA, in contrast with other studies demonstrating improved translation using the former approach. However, a number of factors differ between studies including the type of encoded transgene, the route of administration, and method of formulation. Most studies reporting large increases in translation due to pseudouridine-modifications did so using intracellular reporter genes such as luciferase or green fluorescent protein,[37,67,68] which are less likely to induce ER stress-related shutdown of gene expression. For studies that did evaluate the effect of pseudouridine modification on protein secretion, those reporting enhancement did so within the context of dendritic cell transfections *in vitro*[68] or following intraperitoneal (i.p.) injection *in vivo* with the same formulation.[38] In contrast, those reporting no enhancement or reduction in protein secretion *in vivo* associated with pseudouridine modification did so using LNP formulation and i.v. injection[69] or using TransIT formulation and i.p.injection.[70] We used IM injection of NLC-formulated modified or unmodified mRNA and did not observe an improvement in antibody secretion into the serum of mice nor any difference in expression kinetics.

Although a repRNA strategy offers advantages over non-replicating mRNA for expression of antibodies following IM administration, significant improvements in protein secretion may still be needed for optimal expression in larger animals. While we were able to demonstrate protection in mice when repRNA was administered before the enhancing effects of IFNAR1-blockade, 7 or 5 days prior to challenge, protection following RNA administration 1 day before or after challenge was facilitated by temporary blockade of IFNAR1, with waning antibody concentrations observed when RNA was administered 3 days after challenge (4 days after IFNAR1 blockade), resulting in no protective efficacy. The latter observation is likely due to administration of repRNA at a later time following IFNAR1 blockade combined with increasing ZIKV viremia depleting the amount of measurable ZIKV-117 antibody. However, the observation that mice receiving IFNAR1 blockade 1 day prior to IM injections with ZIKV-117 repRNA exhibited relatively high concentrations of ZIKV-117 (e.g., 7.5 μg/mL), indicates that muscle cells can achieve high levels of protein secretion. The presence of intact type I IFN signaling presumably restricts the replication and translation steps of repRNA-mediated gene expression, which limits antibody levels. We are actively pursuing genetic strategies that modify the repRNA to antagonize innate immunity more effectively and augment protein secretion and IgG accumulation from muscle cells.

In summary, we have optimized the expression of human IgG from repRNA to enable production of protective levels in mice following intramuscular administration from 7 days before and up to 1 day after viral challenge. If we can successfully translate this approach into larger animals and eventually humans, it may become possible to deploy inhibitory antibodies in response to epidemics. Of course, such an approach requires a complementary, rapid antibody discovery platform against emerging pathogens, many of which are under active development.

MATERIALS AND METHODS

Cells and Viruses

293T, BHK21, and Vero cells (American Type Culture Collection, Rockville, MD, USA) were maintained at 37°C in 5% CO_2 in Dulbecco's minimal essential medium (DMEM) containing 10% (vol/vol) heat-inactivated fetal bovine serum (FBS), sodium pyruvate (1 mM), penicillin (100 U/mL), and streptomycin (100 μg/mL). All cell lines were prescreened for mycoplasma contamination. Propagation of ZIKV-MA (GenBank: MG758786.1), a mouse-adapted isolate of ZIKV strain Dakar 41525 mouse (Senegal, 1984; GenBank: KU955591), as well as parental ZIKV Dakar 41525, and ZIKV FSS13025, was described previously.[26,40] Briefly, ZIKV stocks were propagated in Vero cell monolayer cultures, and cell supernatants were harvested 66 to 72 h after inoculation. Virus stocks were titrated by focus forming assay (FFA) or plaque assay on Vero cell monolayers, aliquoted, and stored at −80°C until use.

Plasmid Constructs

A plasmid encoding the Venezuelan equine encephalitis virus (strain TC-83) under the control of a T7 promoter (pT7-VEE-Rep) was described previously.[26] All cloning steps below used a Gibson assembly method with 40-bp homologous overlaps (SGI-DNA). ZIKV-117 (IgG1 isotype) with T2A or IRES DNA sequences was synthesized using gblocks (IDT) and cloned between PflFI and SacII sites of pT7-VEE-Rep. For screening of various IRES sequences, a fragment encoding H chain nanoluciferase was synthesized with 2 BspQI restriction sites between the 2 genes for universal insertion of heterologous sequences. This fragment was inserted between the PflFI and SacII of pT7-VEE-Rep. Synthesized IRES sequences then were inserted between the BspQI sites. For the mRNA control plasmids, a fragment encoding a T7 promoter, genes encoding ZIKV-117 antibody flanked by previously described 5′ and 3′ UTRs and a poly(A) tail was inserted between MluI and NotI sites of pT7-VEE-Rep, replacing the entire VEE-Rep sequence.

RNA *In Vitro* Transcription and Capping

To generate linear templates for RNA transcription, we cut repRNA or mRNA plasmid DNA by restriction digest using NotI or BspQI enzymes (New England Biolabs), respectfully, and purified using phenol-chloroform extraction and sodium acetate precipitation. RNA was transcribed using T7 polymerase, RNase inhibitor, pyrophosphatase enzymes (Aldevron), and reaction buffer. RNA transcripts were capped with vaccinia virus capping enzyme using GTP and S-adenosyl-methionine (New England Biolabs) as substrates to create a cap-0 structure. RNA was purified using LiCl precipitation. To generate pseudouridine-modified RNAs, was replaced 100% of uridine with pseudouridine in the reaction mixture and transcribed and capped as described above.

Formulation Production

The NLC nanoparticle formulation was manufactured as previously described.[26] The oil phase is composed of squalene (the liquid-phase of the oil core), glyceryl trimyristate (Dynasan 114; the solid-phase of the oil core), a non-ionic sorbitan ester surfactant (sorbitan monostearate [Span 60]), and the cationic lipid DOTAP (N-[1-(2,3-Dioleoyloxy) propyl]-N,N,N-trimethylammonium chloride). The aqueous phase is a 10 mM sodium citrate trihydrate buffer containing the non-ionic PEGylated surfactant Tween 80. Separately, the two phases were heated and equilibrated to 60°C in a bath sonicator. Following complete dissolution of the solid components, the oil and aqueous phases were mixed at 5,000 rpm in a high-speed laboratory emulsifier (Silverson Machines) to produce a crude mixture containing micron-sized oil droplets. Further particle size reduction was achieved by homogenization in a M-110P microfluidizer (Microfluidics). The crude mixture was processed at 30,000 psi for ten discrete microfluidization passes. The final pH was between 5.5 and 6.0. Formulations were filtered with a 0.2 μm polyethersulfone membrane syringe filter and stored at 2°C to 8°C. RNA was complexed with NLC at a nitrogen-to-phosphate ratio of 5, diluting NLC in 10 mM citrate buffer and RNA in a 20% sucrose solution and complexing on ice for 30 min prior to use.

Nanoluciferase Assays

Candidate RNAs were serially diluted, complexed with lipofectamine 2000 using the manufacturer's instructions, and added to white

96-well plates. BHK cells then were added to each well, and 16 to 24 h after transfection, Nano-Glo Luciferase Assay Reagent (Promega) was added to each well, and luminescence was measured.

Virus Neutralization Assays

Fifty percent plaque-reduction neutralization tests ($PRNT_{50}$) were performed on Vero cell monolayers as previously described[71] using the Cambodian ZIKV strain FSS 13025 as the control virus. Briefly, ZIKV FSS 13025 (200 PFU) was mixed with serial dilutions of heat-inactivated serum in DMEM containing 1% FBS. Samples then were incubated at 37°C for 1 h, transferred to 90% confluent monolayers of Vero cells in 6-well plates (Costar), and incubated at 37°C for 1 h. An overlay containing 1% agarose in DMEM with 1% non-essential amino acids, 1% L-glutamine, and 1% gentamycin then was pipetted into each well, and plates were incubated for 3 days at 37°C. Cells were fixed in 10% formaldehyde, and plaques visualized following crystal violet staining.

ELISAs

The amount of human mAb in serum was detected using a capture ELISA with a standard curve of recombinant anti-ZIKV mAb ZIKV-117 or an IgG1 isotype-matched control anti-influenza mAb, 5J8. Briefly, plates were coated with 2 μg/mL of goat anti-human kappa or goat anti-human lambda antibodies cross-absorbed against mouse IgG at 4°C overnight. Plates were blocked using 2% BSA in PBS for 1 h at 37°C and then incubated for 1 h at 4°C with serial dilutions of heat-inactivated mouse serum in parallel with a serial dilution of a known quantity of ZIKV-117 hIgG1 protein. After washing, bound antibody was detected using HRP-conjugated goat anti-human Fc multiple species cross-absorbed (1:2,000; Southern Biotech) for 1 h at 4°C. Plates were developed using TMB substrate (Thermo Fisher Scientific), and the reaction was stopped with H_2SO_4. ELISA plates were read using a TriBar LB941 plate reader (Berthold Technologies). The optical density values from the known quantity of ZIKV-117 hIgG1 were fitted to a standard curve and compared to the optical density values of serum to determine the concentration of ZIKV-117 hIgG1.

Viremia Measurements

Blood was drawn from ZIKV-infected mice at various time points, allowed to clot at room temperature, and serum was separated by centrifugation. Viral RNA was isolated using the 96-well Viral RNA kit (Epigenetics), as described by the manufacturer. ZIKV RNA levels were determined by TaqMan one-step quantitative reverse transcriptase PCR (qRT-PCR), as described previously[72]. A published primer set[72] was used to detect ZIKV RNA: forward 5′-CCACCAATGTTCTCTT GCAGACATATTG-3′; reverse 5′-TTCGGACAGCCGTTGTCCAA CACAAG-3′; Probe 5′-/56-FAM/AGCCTACCT/ZEN/TGACAAG CAGTC/3IABkFQ/-3′ (Integrated DNA Technologies). For quantification of infectious ZIKV in serum, virus titer was determined by plaque assay as follows: serial dilutions of serum were added to 90% confluent monolayers of Vero cells in 6-well plates (Costar) and incubated at 37°C for 1 h. An overlay containing 1% agarose in DMEM with 1% non-essential amino acids, 1% L-glutamine, and 1% gentamycin then was pipetted into each well, and plates were incubated for 3 days at 37°C. Cells then were fixed in 10% formaldehyde, and plaques were visualized following crystal violet staining.

Mouse Studies

All animal studies were approved by the Infectious Disease Research Institute or Washington University School of Medicine (assurance number A3381-01) Institutional Animal Care and Use Committee. The facility where animal studies were conducted is accredited by the Association for Assessment and Accreditation of Laboratory Animal Care, International and follows guidelines set forth by the Guide for the Care and Use of Laboratory Animals, National Research Council, 2011. Blood was obtained as approved by cheek or retro-orbital bleeding. Virus inoculations were performed under anesthesia that was induced and maintained with ketamine hydrochloride and xylazine, and all efforts were made to minimize animal suffering. Mice were non-specifically and blindly distributed into respective groups. WT female C57BL/6 mice (4 weeks of age) were purchased from Jackson Laboratory or Charles River. For studies involving ZIKV challenge, mice were treated with 2 mg of an IFNAR1-blocking antibody (MAR1-5A3, Leinco Technologies) by i.p. injection 1 day before virus inoculation, and in some cases (as indicated in the figure legends) additional 0.5 mg doses of anti-IFNAR1 were administered 1 and 4 days after ZIKV inoculation. Mice were inoculated with 40 μg of RNA using by an IM route (into each quadricep and hamstring muscle groups) with four injections of 50 μL of RNA/NLC complex per injection. For most ZIKV infections, mice were inoculated by a subcutaneous (via footpad) route with 10^3 FFU of ZIKV-MA in a volume of 30 μL of PBS. In other studies, mice were inoculated via i.p. route with 10^5 PFU of parental ZIKV strain Dakar 41525. For survival studies, mice were monitored for 21 days.

Data Analysis

Statistical analysis was performed using GraphPad Prism software (version 7.0c) and RStudio (version 0.99.491). Data distribution and variance were evaluated for normality and similarity with or without transformation by qqplot and boxplot analyses. One-way and two-way ANOVAs with Tukey's and Bonferroni's multiple comparison tests, as well as Mann-Whitney and log-rank tests, were used, as described in the figure legends.

SUPPLEMENTAL INFORMATION

Supplemental Information can be found online at https://doi.org/10.1016/j.omtm.2020.06.011.

AUTHOR CONTRIBUTIONS

Conceptualization, J.H.E., N.V.H., S.G.R., M.S.D., J.E.C., R.H.C.; Methodology, J.H.E., J.A., A.P.K., E.V., J.F.-S., B.G., R.G.B., L.B.T., J.G., Q.T., L.A.D., M.S.D., J.E.C., R.H.C., N.V.H.; Investigation, J.H.E., J.A., J.F.-S., A.P.K., E.V., B.G., R.G.B., J.G., Q.T., L.A.D.; Writing – Original Draft, J.H.E., J.A.; Writing – Review & Editing, J.H.E., J.A., E.V., L.B.T., R.H.C., M.S.D., J.E.C.; Funding Acquisition,

S.G.R., M.S.D., J.E.C.; Supervision, L.B.T., M.S.D., J.E.C., R.H.C., R.N.C., S.G.R., N.V.H.

CONFLICTS OF INTERESTS

J.E.C. has served as a consultant for Takeda Vaccines, Sanofi Pasteur, Pfizer, and Novavax, is on the Scientific Advisory Boards of CompuVax and Meissa Vaccines, and is Founder of IDBiologics. M.S.D. is a consultant for Inbios and Emergent BioSolutions and on the Scientific Advisory Board of Moderna. IDRI has applied for a patent related to the NLC formulation. All other authors declare no competing interests.

ACKNOWLEDGMENTS

This study was supported by Defense Advanced Research Projects Agency grant HR0011-18-2-0001 and National Institutes of Health grant R01 AI127828. J.H.E. is supported by fellowships from the Washington Research Foundation and NIH 1F32AI136371.

REFERENCES

1. Van Hoecke, L., and Roose, K. (2019). How mRNA therapeutics are entering the monoclonal antibody field. J. Transl. Med. *17*, 54.
2. Both, L., Banyard, A.C., van Dolleweerd, C., Wright, E., Ma, J.K., and Fooks, A.R. (2013). Monoclonal antibodies for prophylactic and therapeutic use against viral infections. Vaccine *31*, 1553–1559.
3. Kelley, B. (2009). Industrialization of mAb production technology: the bioprocessing industry at a crossroads. MAbs *1*, 443–452.
4. Kose, N., Fox, J.M., Sapparapu, G., Bombardi, R., Tennekoon, R.N., Dharshan de Silva, A., Elbashir, S.M., Theisen, M.A., Humphris-Narayanan, E., Ciaramella, G., et al. (2019). A lipid-encapsulated mRNA encoding a potently neutralizing human monoclonal antibody protects against chikungunya infection. Science Immunology *35*, 6647.
5. Esquivel, R.N., Patel, A., Kudchodkar, S.B., Park, D.H., Stettler, K., Beltramello, M., Allen, J.W., Mendoza, J., Ramos, S., Choi, H., et al. (2019). In Vivo Delivery of a DNA-Encoded Monoclonal Antibody Protects Non-human Primates against Zika Virus. Mol. Ther. *27*, 974–985.
6. Tiwari, P.M., Vanover, D., Lindsay, K.E., Bawage, S.S., Kirschman, J.L., Bhosle, S., Lifland, A.W., Zurla, C., and Santangelo, P.J. (2018). Engineered mRNA-expressed antibodies prevent respiratory syncytial virus infection. Nat. Commun. *9*, 3999.
7. Thran, M., Mukherjee, J., Pönisch, M., Fiedler, K., Thess, A., Mui, B.L., Hope, M.J., Tam, Y.K., Horscroft, N., Heidenreich, R., et al. (2017). mRNA mediates passive vaccination against infectious agents, toxins, and tumors. EMBO Mol. Med. *9*, 1434–1447.
8. Andrews, C.D., Luo, Y., Sun, M., Yu, J., Goff, A.J., Glass, P.J., Padte, N.N., Huang, Y., and Ho, D.D. (2017). In Vivo Production of Monoclonal Antibodies by Gene Transfer via Electroporation Protects against Lethal Influenza and Ebola Infections. Mol. Ther. Methods Clin. Dev. *7*, 74–82.
9. Muthumani, K., Block, P., Flingai, S., Muruganantham, N., Chaaithanya, I.K., Tingey, C., Wise, M., Reuschel, E.L., Chung, C., Muthumani, A., et al. (2016). Rapid and Long-Term Immunity Elicited by DNA-Encoded Antibody Prophylaxis and DNA Vaccination Against Chikungunya Virus. J. Infect. Dis. *214*, 369–378.
10. Muthumani, K., Flingai, S., Wise, M., Tingey, C., Ugen, K.E., and Weiner, D.B. (2013). Optimized and enhanced DNA plasmid vector based in vivo construction of a neutralizing anti-HIV-1 envelope glycoprotein Fab. Hum. Vaccin. Immunother. *9*, 2253–2262.
11. Suscovich, T.J., and Alter, G. (2015). In situ production of therapeutic monoclonal antibodies. Expert Rev. Vaccines *14*, 205–219.
12. Deal, C.E., and Balazs, A.B. (2015). Vectored antibody gene delivery for the prevention or treatment of HIV infection. Curr. Opin. HIV AIDS *10*, 190–197.
13. Schlake, T., Thran, M., Fiedler, K., Heidenreich, R., Petsch, B., and Fotin-Mleczek, M. (2019). mRNA: A Novel Avenue to Antibody Therapy? Mol. Ther. *27*, 773–784.
14. Schlake, T., Thess, A., Thran, M., and Jordan, I. (2019). mRNA as novel technology for passive immunotherapy. Cell. Mol. Life Sci. *76*, 301–328.
15. Sabnis, S., Kumarasinghe, E.S., Salerno, T., Mihai, C., Ketova, T., Senn, J.J., Lynn, A., Bulychev, A., McFadyen, I., Chan, J., et al. (2018). A Novel Amino Lipid Series for mRNA Delivery: Improved Endosomal Escape and Sustained Pharmacology and Safety in Non-human Primates. Mol. Ther. *26*, 1509–1519.
16. Stadler, C.R., Bähr-Mahmud, H., Celik, L., Hebich, B., Roth, A.S., Roth, R.P., Karikó, K., Türeci, Ö., and Sahin, U. (2017). Elimination of large tumors in mice by mRNA-encoded bispecific antibodies. Nat. Med. *23*, 815–817.
17. Pardi, N., Secreto, A.J., Shan, X., Debonera, F., Glover, J., Yi, Y., Muramatsu, H., Ni, H., Mui, B.L., Tam, Y.K., et al. (2017). Administration of nucleoside-modified mRNA encoding broadly neutralizing antibody protects humanized mice from HIV-1 challenge. Nat. Commun. *8*, 14630.
18. Tetteh, E.K., and Morris, S. (2014). Evaluating the administration costs of biologic drugs: development of a cost algorithm. Health Econ. Rev. *4*, 26.
19. Geall, A.J., Verma, A., Otten, G.R., Shaw, C.A., Hekele, A., Banerjee, K., Cu, Y., Beard, C.W., Brito, L.A., Krucker, T., et al. (2012). Nonviral delivery of self-amplifying RNA vaccines. Proc. Natl. Acad. Sci. USA *109*, 14604–14609.
20. Cugola, F.R., Fernandes, I.R., Russo, F.B., Freitas, B.C., Dias, J.L., Guimarães, K.P., Benazzato, C., Almeida, N., Pignatari, G.C., Romero, S., et al. (2016). The Brazilian Zika virus strain causes birth defects in experimental models. Nature *534*, 267–271.
21. Anaya, J.-M., Rodríguez, Y., Monsalve, D.M., Vega, D., Ojeda, E., González-Bravo, D., Rodríguez-Jiménez, M., Pinto-Díaz, C.A., Chaparro, P., Gunturiz, M.L., et al. (2017). A comprehensive analysis and immunobiology of autoimmune neurological syndromes during the Zika virus outbreak in Cúcuta, Colombia. J. Autoimmun. *77*, 123–138.
22. Rasmussen, S.A., Jamieson, D.J., Honein, M.A., and Petersen, L.R. (2016). Zika virus and birth defects—reviewing the evidence for causality. N. Engl. J. Med. *374*, 1981–1987.
23. Pinto-Díaz, C.A., Rodríguez, Y., Monsalve, D.M., Acosta-Ampudia, Y., Molano-González, N., Anaya, J.M., and Ramírez-Santana, C. (2017). Autoimmunity in Guillain-Barré syndrome associated with Zika virus infection and beyond. Autoimmun. Rev. *16*, 327–334.
24. Sapparapu, G., Fernandez, E., Kose, N., Bin Cao, Fox, J.M., Bombardi, R.G., Zhao, H., Nelson, C.A., Bryan, A.L., Barnes, T., et al. (2016). Neutralizing human antibodies prevent Zika virus replication and fetal disease in mice. Nature *540*, 443–447.
25. Hasan, S.S., Miller, A., Sapparapu, G., Fernandez, E., Klose, T., Long, F., Fokine, A., Porta, J.C., Jiang, W., Diamond, M.S., et al. (2017). A human antibody against Zika virus crosslinks the E protein to prevent infection. Nat. Commun. *8*, 14722.
26. Erasmus, J.H., Khandhar, A.P., Guderian, J., Granger, B., Archer, J., Archer, M., Gage, E., Fuerte-Stone, J., Larson, E., Lin, S., et al. (2018). A Nanostructured Lipid Carrier for Delivery of a Replicating Viral RNA Provides Single, Low-Dose Protection against Zika. Mol. Ther. *26*, 2507–2522.
27. Haryadi, R., Ho, S., Kok, Y.J., Pu, H.X., Zheng, L., Pereira, N.A., Li, B., Bi, X., Goh, L.T., Yang, Y., and Song, Z. (2015). Optimization of heavy chain and light chain signal peptides for high level expression of therapeutic antibodies in CHO cells. PLoS ONE *10*, e0116878.
28. Ho, S.C.L., Bardor, M., Li, B., Lee, J.J., Song, Z., Tong, Y.W., Goh, L.-T., and Yang, Y. (2013). Comparison of Internal Ribosome Entry Site (IRES) and Furin-2A (F2A) for Monoclonal Antibody Expression Level and Quality in CHO Cells. PLoS One *8*, e63247.
29. Chng, J., Wang, T., Nian, R., Lau, A., Hoi, K.M., Ho, S.C., Gagnon, P., Bi, X., and Yang, Y. (2015). Cleavage efficient 2A peptides for high level monoclonal antibody expression in CHO cells. MAbs *7*, 403–412.

30. Pinkstaff, J.K., Chappell, S.A., Mauro, V.P., Edelman, G.M., and Krushel, L.A. (2001). Internal initiation of translation of five dendritically localized neuronal mRNAs. Proc. Natl. Acad. Sci. USA *98*, 2770–2775.

31. Bochkov, Y.A., and Palmenberg, A.C. (2006). Translational efficiency of EMCV IRES in bicistronic vectors is dependent upon IRES sequence and gene location. Biotechniques *41*, 283–284, 286, 288 passim.

32. Allera-Moreau, C., Delluc-Clavières, A., Castano, C., Van den Berghe, L., Golzio, M., Moreau, M., Teissié, J., Arnal, J.F., and Prats, A.C. (2007). Long term expression of bicistronic vector driven by the FGF-1 IRES in mouse muscle. BMC Biotechnol. *7*, 74.

33. Gross, L., Vicens, Q., Einhorn, E., Noireterre, A., Schaeffer, L., Kuhn, L., Imler, J.L., Eriani, G., Meignin, C., and Martin, F. (2017). The IRES5'UTR of the dicistrovirus cricket paralysis virus is a type III IRES containing an essential pseudoknot structure. Nucleic Acids Res. *45*, 8993–9004.

34. Licursi, M., Christian, S.L., Pongnopparat, T., and Hirasawa, K. (2011). In vitro and in vivo comparison of viral and cellular internal ribosome entry sites for bicistronic vector expression. Gene Ther. *18*, 631–636.

35. Koev, G., Duncan, R.F., Lai, M.M.C., and Hepatitis, C. (2002). Hepatitis C virus IRES-dependent translation is insensitive to an eIF2α-independent mechanism of inhibition by interferon in hepatocyte cell lines. Virology *297*, 195–202.

36. Pan, M., Yang, X., Zhou, L., Ge, X., Guo, X., Liu, J., Zhang, D., and Yang, H. (2012). Duck Hepatitis A virus possesses a distinct type IV internal ribosome entry site element of picornavirus. J. Virol. *86*, 1129–1144.

37. Karikó, K., Muramatsu, H., Welsh, F.A., Ludwig, J., Kato, H., Akira, S., and Weissman, D. (2008). Incorporation of pseudouridine into mRNA yields superior nonimmunogenic vector with increased translational capacity and biological stability. Mol. Ther. *16*, 1833–1840.

38. Karikó, K., Muramatsu, H., Keller, J.M., and Weissman, D. (2012). Increased erythropoiesis in mice injected with submicrogram quantities of pseudouridine-containing mRNA encoding erythropoietin. Mol. Ther. *20*, 948–953.

39. Sheehan, K.C.F., Lai, K.S., Dunn, G.P., Bruce, A.T., Diamond, M.S., Heutel, J.D., Dungo-Arthur, C., Carrero, J.A., White, J.M., Hertzog, P.J., and Schreiber, R.D. (2006). Blocking monoclonal antibodies specific for mouse IFN-alpha/beta receptor subunit 1 (IFNAR-1) from mice immunized by in vivo hydrodynamic transfection. J. Interferon Cytokine Res. *26*, 804–819.

40. Gorman, M.J., Caine, E.A., Zaitsev, K., Begley, M.C., Weger-Lucarelli, J., Uccellini, M.B., Tripathi, S., Morrison, J., Yount, B.L., Dinnon, K.H., 3rd, et al. (2018). An Immunocompetent Mouse Model of Zika Virus Infection. Cell Host Microbe *23*, 672–685.e6.

41. Smith, D.R., Hollidge, B., Daye, S., Zeng, X., Blancett, C., Kuszpit, K., Bocan, T., Koehler, J.W., Coyne, S., Minogue, T., et al. (2017). Neuropathogenesis of Zika Virus in a Highly Susceptible Immunocompetent Mouse Model after Antibody Blockade of Type I Interferon. PLoS Negl. Trop. Dis. *11*, e0005296.

42. Rule, S., Collins, G.P., and Samanta, K. (2014). Subcutaneous vs intravenous rituximab in patients with non-Hodgkin lymphoma: a time and motion study in the United Kingdom. J. Med. Econ. *17*, 459–468.

43. Pivot, X., Gligorov, J., Müller, V., Curigliano, G., Knoop, A., Verma, S., Jenkins, V., Scotto, N., Osborne, S., and Fallowfield, L.; PrefHer Study Group (2014). Patients' preferences for subcutaneous trastuzumab versus conventional intravenous infusion for the adjuvant treatment of HER2-positive early breast cancer: final analysis of 488 patients in the international, randomized, two-cohort PrefHer study. Ann. Oncol. *25*, 1979–1987.

44. De Cock, E., Pan, Y.I., Tao, S., and Baidin, P. (2014). Time Savings With Transtuzumab Subcutaneous (SC) Injection Verse Trastuzumab Intravenous (IV) Infusion: A Time and Motion Study in 3 Russian Centers. Value Health *17*, A653.

45. De Cock, E., Kritikou, P., Sandoval, M., Tao, S., Wiesner, C., Carella, A.M., Ngoh, C., and Waterboer, T. (2016). Time Savings with Rituximab Subcutaneous Injection versus Rituximab Intravenous Infusion: A Time and Motion Study in Eight Countries. PLoS ONE *11*, e0157957.

46. Maxmen, A. (2019). Two Ebola drugs show promise amid ongoing outbreak. Nature. https://doi.org/10.1038/d41586-019-02442-6.

47. Frolov, I., Hoffman, T.A., Pragai, B.M., Dryga, S.A., Huang, H.V., Schlesinger, S., and Rice, C.M. (1996). Alphavirus-based expression vectors: Strategies and applications. Proc. Natl. Acad. Sci. USA *93*, 11371–11377.

48. Frolov, I., Hoffman, T.A., Prágai, B.M., Dryga, S.A., Huang, H.V., Schlesinger, S., and Rice, C.M. (1996). Alphavirus-based expression vectors: strategies and applications. Proc. Natl. Acad. Sci. USA *93*, 11371–11377.

49. Fros, J.J., and Pijlman, G.P. (2016). Alphavirus infection: Host cell shut-off and inhibition of antiviral responses. Viruses *8*, 166.

50. Bhalla, N., Sun, C., Metthew Lam, L.K., Gardner, C.L., Ryman, K.D., and Klimstra, W.B. (2016). Host translation shutoff mediated by non-structural protein 2 is a critical factor in the antiviral state resistance of Venezuelan equine encephalitis virus. Virology *496*, 147–165.

51. Leitzgen, K., Knittler, M.R., and Haas, I.G. (1997). Assembly of immunoglobulin light chains as a prerequisite for secretion. A model for oligomerization-dependent subunit folding. J. Biol. Chem. *272*, 3117–3123.

52. Roberts, L., and Wieden, H.J. (2018). Viruses, IRESs, and a universal translation initiation mechanism. Biotechnol. Genet. Eng. Rev. *34*, 60–75.

53. Schlatter, S., Stansfield, S.H., Dinnis, D.M., Racher, A.J., Birch, J.R., and James, D.C. (2005). On the optimal ratio of heavy to light chain genes for efficient recombinant antibody production by CHO cells. Biotechnol. Prog. *21*, 122–133.

54. Jiang, Z., Huang, Y., and Sharfstein, S.T. (2006). Regulation of recombinant monoclonal antibody production in chinese hamster ovary cells: a comparative study of gene copy number, mRNA level, and protein expression. Biotechnol. Prog. *22*, 313–318.

55. Li, J., Zhang, C., Jostock, T., and Dübel, S. (2007). Analysis of IgG heavy chain to light chain ratio with mutant Encephalomyocarditis virus internal ribosome entry site. Protein Eng. Des. Sel. *20*, 491–496.

56. Ho, S.C.L., Bardor, M., Feng, H., Mariati, Tong, Y.W., Song, Z., Yap, M.G., and Yang, Y. (2012). IRES-mediated Tricistronic vectors for enhancing generation of high monoclonal antibody expressing CHO cell lines. J. Biotechnol. *157*, 130–139.

57. Gonz lez, R., Andrews, B.A., and Asenjo, J.A. (2002). Kinetic model of BiP- and PDI-mediated protein folding and assembly. J. Theor. Biol. *214*, 529–537.

58. Chusainow, J., Yang, Y.S., Yeo, J.H., Toh, P.C., Asvadi, P., Wong, N.S., and Yap, M.G. (2009). A study of monoclonal antibody-producing CHO cell lines: what makes a stable high producer? Biotechnol. Bioeng. *102*, 1182–1196.

59. Götte, B., Panas, M.D., Hellström, K., Liu, L., Samreen, B., Larsson, O., Ahola, T., and McInerney, G.M. (2019). Separate domains of G3BP promote efficient clustering of alphavirus replication complexes and recruitment of the translation initiation machinery. PLoS Pathog. *15*, e1007842.

60. Barry, G., Fragkoudis, R., Ferguson, M.C., Lulla, A., Merits, A., Kohl, A., and Fazakerley, J.K. (2010). Semliki forest virus-induced endoplasmic reticulum stress accelerates apoptotic death of mammalian cells. J. Virol. *84*, 7369–7377.

61. Vitale, M., Bakunts, A., Orsi, A., Lari, F., Tadè, L., Danieli, A., Rato, C., Valetti, C., Sitia, R., Raimondi, A., et al. (2019). Inadequate BiP availability defines endoplasmic reticulum stress. eLife *8*, 1–17.

62. Lenny, N., and Green, M. (1991). Regulation of endoplasmic reticulum stress proteins in COS cells transfected with immunoglobulin μ heavy chain cDNA. J. Biol. Chem. *266*, 20532–20537.

63. Haas, I.G., and Wabl, M.R. (1984). Immunoglobulin heavy chain toxicity in plasma cells is neutralized by fusion to pre-B cells. Proc. Natl. Acad. Sci. USA *81*, 7185–7188.

64. Bole, D.G., Hendershot, L.M., and Kearney, J.F. (1986). Posttranslational association of immunoglobulin heavy chain binding protein with nascent heavy chains in nonsecreting and secreting hybridomas. J. Cell Biol. *102*, 1558–1566.

65. Prashad, K., and Mehra, S. (2015). Dynamics of unfolded protein response in recombinant CHO cells. Cytotechnology *67*, 237–254.

66. Flingai, S., Plummer, E.M., Patel, A., Shresta, S., Mendoza, J.M., Broderick, K.E., Sardesai, N.Y., Muthumani, K., and Weiner, D.B. (2015). Protection against dengue disease by synthetic nucleic acid antibody prophylaxis/immunotherapy. Sci. Rep. *5*, 12616.

67. Li, B., Luo, X., and Dong, Y. (2016). Effects of Chemically Modified Messenger RNA on Protein Expression. Bioconjug. Chem. *27*, 849–853.

68. Karikó, K., Muramatsu, H., Ludwig, J., and Weissman, D. (2011). Generating the optimal mRNA for therapy: HPLC purification eliminates immune activation and improves translation of nucleoside-modified, protein-encoding mRNA. Nucleic Acids Res. *39*, e142.

69. Kauffman, K.J., Mir, F.F., Jhunjhunwala, S., Kaczmarek, J.C., Hurtado, J.E., Yang, J.H., Webber, M.J., Kowalski, P.S., Heartlein, M.W., DeRosa, F., and Anderson, D.G. (2016). Efficacy and immunogenicity of unmodified and pseudouridine-modified mRNA delivered systemically with lipid nanoparticles in vivo. Biomaterials *109*, 78–87.

70. Thess, A., Grund, S., Mui, B.L., Hope, M.J., Baumhof, P., Fotin-Mleczek, M., and Schlake, T. (2015). Sequence-engineered mRNA Without Chemical Nucleoside Modifications Enables an Effective Protein Therapy in Large Animals. Mol. Ther. *23*, 1456–1464.

71. Beaty, B.J.J., Calisher, C.H.H., and Shope, R.E.E. (1989). Arboviruses. In Diagnostic procedures for viral, rickettsial and chlamydial infections, N.J.J. Schmidt and R.W.W. Emmons, eds. (American Public Health Association), pp. 797–855.

72. Govero, J., Esakky, P., Scheaffer, S.M., Fernandez, E., Drury, A., Platt, D.J., et al. (2016). Zika virus infection damages the testes in mice. Nature *540*, 438–442.